La_2CuSnO_6: A New Perovskite-Related Compound with an Unusual Arrangement of B Cations

Mark T. Anderson and Kenneth R. Poeppelmeier*

Department of Chemistry and the Science and Technology Center for Superconductivity, Northwestern University, Evanston, Illinois 60208

Received November 14, 1990. Revised Manuscript Received January 25, 1991

The structure of La_2CuSnO_6 was determined by Rietveld refinement of time-of-flight powder neutron diffraction data. The structure was solved in space group $P2_1/m$ with unit-cell parameters $a = 8.510$ (1), $b = 7.815$ (1), $c = 7.817$ (1) Å, and $\beta = 91.15$ (1)°. The structure is best described as a $2a_p \times 2a_p \times 2a_p$ distorted perovskite with an unusual arrangement of B cations that produces distinct copper–oxygen and tin–oxygen layers. The structural aspects are similar to the high-temperature cuprate superconductors. The magnetic susceptibility versus temperature profile indicates the compound is not a superconductor above 5 K. The phase diagram of the $LaO_{1.5}$–CuO–SnO_2 system was determined at 980 °C in air. La_2CuSnO_6 is the only ternary compound in the system.

Introduction

The important role that copper–oxygen layers have in high-temperature superconductors ($T_c > 35$ K) was realized after the report on the La-Ba-Cu-O[1] system by Bednorz and Müller in 1986. Although no theory of the mechanism of high-temperature superconductivity has gained complete acceptance, it is clear that copper–oxygen layers largely determine the electronic properties of the cuprate superconductors.

The prototype members of these families of superconductors are $La_{2-x}M_xCuO_{4-\delta}$[2,3] (M = Ca, Sr, Ba), $Nd_{2-x}Ce_xCuO_{4+\delta}$,[4] $YBa_2Cu_3O_{7-y}$,[5] $(Tl,Bi)_m(Ba,Sr)_2Ca_{n+1}Cu_nO_{m+2n+2}$[6,7] ($m$, n = integer), $Pb_2Sr_2LnCu_3O_{8+\delta}$[8] (Ln = lanthanide), and $La_{2-x}Sr_xCaCu_2O_6$.[9] All can be described as an intergrowth of AO rock salt layers with ABO_{3-x} perovskite units. They have the general formula $(AO)_m(ABO_{3-x})_n$, where m and n are integers and B is copper. The common feature of these compounds is that they possess copper–oxygen layers that have been oxidized or reduced. The structural similarity of these compounds directed our search for new superconductors.

Our goal was the synthesis of layered copper oxides. More specifically we focused on the synthesis of $A_2BB'O_6$ compounds that contain distinct $BO_{4/2}$[10] and $B'O_{4/2}$ layers, where B is copper and B′ is a nonmagnetic d^{10} or d^0 cation.

A barrier to the synthesis of these compounds is that the B and B′ cations are generally arranged such that the $BO_{6/2}$ perovskite framework contains only mixed $(B,B')O_{4/2}$ layers. In the two arrangements commonly observed the cations are either ordered between alternate close packed AO_3 layers (…AO_3–B–AO_3–B′–AO_3… sequence, commonly refered to as an "ordered perovskite structure") or completely disordered.[11] Neither arrangement produces compounds with distinct $CuO_{4/2}$ layers. The importance of these layers has been underscored by many experiments that have examined the effect of partial substitution of other elements,[12] such as Zn,[13] Fe,[13] Co,[14] Ni,[14] Ag,[15] and Pd,[16] into the copper–oxide planes (or chains) of high-temperature superconductors. The results demonstrated that no substitution reproducibily increased T_c; in fact these substitutions diminished T_c or destroyed the superconducting state even when the concentration of the dopant was quite low (<5%). Thus, the challenge was to synthesize compounds with distinct $CuO_{4/2}$ and $B'O_{4/2}$ layers.

By the use of copper and tin as B and B′ cations, the perovskite-related compound La_2CuSnO_6 with the desired two-dimensional $CuO_{4/2}$ layers has been synthesized. The structure is quite rare in perovskites that are stoichiometric in oxygen. We report on the structure and the crystal chemistry of this compound and the phase diagram of the $LaO_{1.5}$–CuO–SnO_2 system.

---

[1] Bednorz, J. G.; Müller, K. A. *Z. Phys. B—Condensed Matter* **1986**, *64*, 189.

[2] (a) Uchida, S.; Takagi, H.; Kitazawa, K.; Tanaka, S. *Jpn. J. Appl. Phys.* **1987**, *26*, L1. (b) Takagi, H.; Uchida, S.; Kitazawa, K.; Tanaka, S. *Jpn. J. Appl. Phys.* **1987**, *26*, L123.

[3] Cava, R. J.; van Dover, R. B.; Batlogg, B.; Rietman, E. A. *Phys. Rev. Lett.* **1987**, *58*(4), 408.

[4] Tokuza, Y.; Takagi, H.; Uchida, S. *Nature* **1989**, *337*, 345.

[5] (a) Wu, M. K.; Ashburn, J. R.; Torng, C. J.; Hor, P. H.; Meng, R. L.; Gao, L.; Huang, Z. J.; Wang, Y. Q.; Chu, C. W. *Phys. Rev. Lett.* **1987**, *58*(9), 908. (b) Beno, M. A.; Soderholm, D. W.; Capone, D. W.; Jorgensen, J. D.; Schuller, K. I.; Serge, C. U.; Zhang, K.; Grace, J. D. *Appl. Phys. Lett.* **1987**, *51*, 57.

[6] (a) Sheng, Z. Z.; Hermann, A. M. *Nature* **1988**, *332*, 55. (b) Subramanian, M. A.; Torardi, C. C.; Calabrese, J. C.; Gopalakrishnan, J.; Morrissey, J. J.; Askew, T. R.; Flippen, R. B.; Chowdhry, U.; Sleight, A. W. *Nature* **1988**, *332*, 420.

[7] (a) Chu, C. W.; Bechtold, J.; Gao, L.; Hor, P. H.; Huang, Z. J.; Meng, R. L.; Sun, Y. Y.; Wang, Y. Q.; Xue, Y. Y. *Phys. Rev. Lett.* **1988**, *60*(10), 941. (b) Hazen, R. M.; Prewitt, C. T.; Angel, R. J.; Ross, N. L.; Finger, L. W.; Hadidiacos, C. G.; Veblen, D. R.; Heaney, P. J.; Hor, P. H.; Meng, R. L.; Sun, Y. Y.; Wang, Y. Q.; Xue, Y. Y.; Huang, Z. J.; Gao, L.; Bechtold, J.; Chu, C. W. *Phys. Rev. Lett.* **1988**, *60*(12), 1174.

[8] Cava, R. J.; Batlogg, B.; Krajewski, J. J.; Rupp, L. W.; Schneemeyer, L. F.; Siegrist, T.; vanDover, R. B.; Marsh, P.; Peck, W. F., Jr.; Gallagher, P. K.; Glarum, S. H.; Marshall, J. H.; Farrow, R. C.; Waszczak, J. V.; Hull, R.; Trevor, P. *Nature* **1988**, *336*, 211.

[9] Cava, R. J.; Batlogg, B.; vanDover, R. B., Krajewski, J. J.; Waszczak, J. V.; Fleming, R. M.; Peck, W. F.; Rupp, L. W.; Marsh, P.; James, A. C. W. P.; Schneemeyer, L. F. *Nature* **1990**, *345*, 602.

[10] In this notation the first subscripted number refers to the number of oxygen atoms around the cation and the second to the number of cations around each oxygen atom. Note that these numbers depend upon what structural unit is being discussed, for example, layers ($BO_{4/2}$), chains ($BO_{2/2}$), octahedra ($BO_{6/2}$), etc.

[11] Goodenough, J. B.; Longo, J. M. In *Landolt-Börnstein, Numerical Data and Functional Relationships in Science and Technology*; Hellwege, K.-H., Ed.; Springer Verlag: Berlin, 1970; Group III/Vol. 4a, pp 131-147.

[12] Williams, J. M.; Beno, M. A.; Carlson, K. D.; Geiser, U.; Ivy Kao, H. C.; Kini, A. M.; Porter, L. C.; Schultz, A. J.; Thorn, J. T.; Wang, H. H.; Whangbo, M.-H.; Evain, M. *Acc. Chem. Res.* **1988**, *21*(1), 1.

[13] See, for example: Bordet, P.; Hodeau, J. L.; Strobel, P.; Marezio, M.; Santoro, A. *Solid State Commun.* **1988**, *66*, 435.

[14] See, for example: Tarascon, J. M.; Greene, L. H.; Bagley, B. G.; McKinnon, W. R.; Barboux, P.; Hull, G. W. In *Novel Superconductivity*; Proceedings: International Workshop on Novel Mechanisms of Superconductivity, Berkely, CA, 22–26 June 1987; Wolf, S. A., Kresin, V. Z., Eds.; Plenum: New York, 1987; p 705.

[15] Cahen, D.; Schwartz, M.; Reich, S.; Felner, I. *Inorg. Chem.* **1987**, *26*, 3653.

[16] Ferey, G.; Le Bail, A.; Laligant, Y.; Hervieu, M.; Raveau, B.; Sulpice, A.; Tournier, R. *J. Solid State Chem.* **1988**, *73*, 610.

0897-4756/91/2803-0476$02.50/0

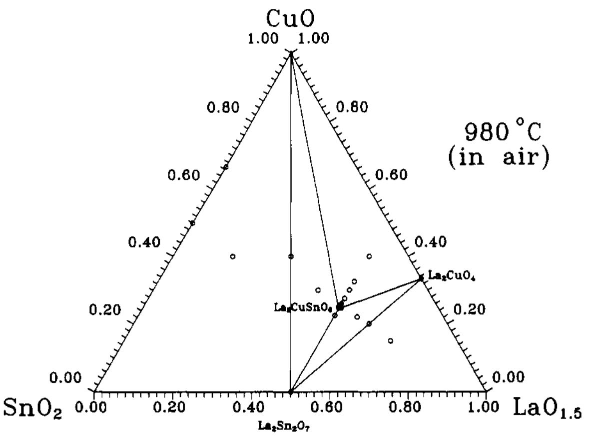

Figure 1. Subsolidus phase diagram of the $LaO_{1.5}$–CuO–SnO_2 system determined at 980 °C in air.

Experimental Section

Sample Preparation. The samples used for the phase diagram determination were prepared by the solid-state reaction of the appropriate ratios of (Aldrich) lanthanum oxide (99.999%), tin(IV) oxide (99.995+%), and copper(II) oxide (99.999%). The reagents were heated in air before use and cooled in a desiccator to remove any traces of water or carbonate. The starting materials were ground and fired in high-density alumina boats for 1 day. The samples were then quenched in air, ground, pressed into pellets, and fired at 980 °C in air. This process was repeated several times. Total reaction times ranged from 7 to 48 days. The samples in the copper-rich part of the diagram required much less time to react than the samples in the tin- or lanthanum-rich areas.

The La_2CuSnO_6 samples for X-ray and neutron diffraction were prepared in a similar manner. To avoid contamination from the alumina boat, the samples were heated at 980 °C, which is well below the liquidus (>1200 °C) of La_2CuSnO_6. At this temperature a minimum reaction time of about 21 days was required to achieve a single phase.

X-ray Diffraction. A Rigaku diffractometer with nickel-filtered Cu Kα radiation was used to perform powder X-ray diffraction (XRD) measurements. The progress of all of the reactions was monitored by XRD. An X-ray diffraction data set suitable for Rietveld[17] refinement was collected on a polycrystalline sample of La_2CuSnO_6. A diffractometer equipped with a LiF monochromator to provide Cu Kα_1 radiation was used for the collection. A 2θ scan from 9° to 85° with a step of 0.01° and a 30-s collection time at each step was employed to collect the diffraction data.

Neutron Diffraction. The Intense Pulsed Neutron Source at Argonne National Laboratory was used to collect time-of-flight data on a polycrystalline sample of La_2CuSnO_6. The sample was at room temperature and ambient pressure during the collection. Approximately 9 g of the sample was contained in a thin-walled vanadium can for the 12-h collection. The data from d = 0.633 to 2.967 Å were analyzed by the Rietveld method.[18,19] Sixty-three parameters were refined. The parameters refined included scale factor, background, peak shape, unit-cell and positional parameters, and isotropic thermal factors. The coherent scattering lengths used for La, Cu, Sn, and O were 8.24, 7.72, 6.23, and 5.80 fm respectively.[20]

Results

$LaO_{1.5}$–CuO–SnO_2 Subsolidus Phase Diagram. The phase diagram of the $LaO_{1.5}$–CuO–SnO_2 system was determined at 980 °C in air. The samples used to determine the diagram had the compositions indicated by an open circle in Figure 1. For each composition, mixtures of lanthanum oxide, copper(II) oxide, and tin(IV) oxide were reacted until equilibrium was reached. Equilibrium was assumed to have been reached when three or fewer solid phases were observed in the powder X-ray diffraction pattern, and the pattern (including the relative intensities of the Bragg peaks) had not changed over a 1-week period. The phases present at each composition were identified by powder X-ray diffraction methods.

Pseudobinary Systems. In the $LaO_{1.5}$–CuO system the well-known compound La_2CuO_4[21] was formed. The compound can be described as a distorted (orthorhombic) K_2NiF_4 structure,[22] *Abma* (No. 64), with a = 5.406, b = 5.370, and c = 13.15 Å. The lanthanum cuprates $LaCuO_2$,[23] $LaCuO_3$,[24] and $La_{n+1}Cu_nO_{3n+1-y}$[25] ($n > 1$), which have not been reported to be stable under the conditions of this investigation, were not detected by X-ray diffraction methods in this study.

In the $LaO_{1.5}$–SnO_2 system the previously reported compound $La_2Sn_2O_7$[26] was formed. The compound has the cubic pyrochlore structure,[27] *Fd3m* (No. 227), and has a unit-cell parameter a_0 = 10.702 Å. No reports of other compounds in this system were found.

No pseudobinary compounds were found in the CuO–SnO_2 system, which was studied up to 1200 °C. No reports of pseudobinary compounds in this system were found, but SnO_2 was reported to have a very slight solubility[28] (~1%) in CuO at 1200 °C.

Ternary System. The only ternary compound present in the $LaO_{1.5}$–CuO–SnO_2 system at 980 °C in air was La_2CuSnO_6. The compound was found to be compatible with CuO, La_2CuO_4, and $La_2Sn_2O_7$. The system was studied at temperatures up to 1050 °C; the phases present and the phase relationships were the same as at 980 °C.

Characterization and Properties of La_2CuSnO_6. La_2CuSnO_6 was initially characterized by energy-dispersive X-ray analysis (EDAX). Approximately 25 individual crystallites (typically 1–2 μm wide) were analyzed. The crystallites were taken from a sample in which the La:Cu:Sn ratio was 2:1:1. The percentages of the metal atoms were determined to be 50.1 (6)% lanthanum, 26.1 (4)% copper, and 23.8 (5)% tin. These values are within 3 standard deviations of the calculated percentages of 50.0%, 25.0%, and 25.0%, respectively.

The oxygen content of La_2CuSnO_6 was determined to be 6.00 ± 0.02 based on thermogravimetric analysis. The measured oxygen content was consistent with tetravalent tin and divalent copper. The oxygen content of the sample did not change when the sample was heated from 25 to 1000 °C and cooled to 25 °C in flowing oxygen. The possibility of a phase transition from monoclinic to cubic symmetry exists, but no phase transitions were detected by differential scanning calorimetry in the temperature range −180 to 600 °C. Magnetic susceptibility measure-

---

[17] Wiles, D. B.; Sakthivel, A.; Young, R. A. *Rietveld Analysis Program DBW3.2S*; School of Physics, Georgia Institute of Technology, 1987.

[18] Von Dreele, R. B.; Jorgensen, G. D.; Windsor, C. G. *J. Appl. Crystallogr.* **1982**, *15*, 581.

[19] Rotella, F. J.; Richardson, J. W., Jr. *Workshop on Neutron Scattering Data Analysis 1986*; IOP Publishing Ltd.: Bristol, UK, 1986; Chapter 1.

[20] Jacobson, A. J.; Tofield, B. C.; Fender, B. E. F. *J. Phys. C* **1973**, *6*, 1615.

[21] Grande, B.; Müller-Buschbaum, H.; Schweizer, M. *Z. Anorg. Allg. Chem.* **1977**, *428*, 120.

[22] Foex, M.; Mancheron, A.; Line, M. *C. R. Acad. Sci.* **1960**, *250*, 3027.

[23] Haas, H.; Kordes, E. *Z. Kristallogr.* **1969**, *129*, 259.

[24] Demazeau, G.; Parent, C.; Pouchard, M.; Hagenmuller, P. *Mater. Res. Bull.* **1972**, *7*, 913.

[25] De Leeuw, D. M.; Mutsaers, A. H. A.; Geelen, G. P. J.; Langereis, C. *J. Solid State Chem.* **1989**, *80*, 276–285.

[26] McCauley, R. A. *J. Appl. Phys.* **1980**, *51*(1), 290.

[27] Whinfrey, C. G.; Eckart, D. W.; Tauber, A. *J. Am. Chem. Soc.* **1960**, *82*, 2695.

[28] Pasternak, M. P.; Taylor, R. D. *Solid State Commun.* **1990**, *73*(1), 33.

Table I. Indexed X-ray Diffraction Pattern of La_2CuSnO_6 (Monoclinic; $P2_1/m$ (No. 11); a = 8.506 (1), b = 7.811 (1), c = 7.814 (1) Å, β = 91.14 (1)°)

$h\ k\ l$	d_{calc}[a]	d_{obs}	I/I_0[b]	$h\ k\ l$	d_{calc}	d_{obs}	I/I_0
2 0 0	4.252	4.252	1	−2 2 4	1.6260	1.6261	9
0 2 0/0 0 2	3.906	3.905	3	−2 4 2	1.6208	1.6209	17
2 1 0	3.735	3.735	2	2 4 2	1.6107	1.6106	21
−1 0 2	3.577	3.577	5	4 3 1	1.6064	1.6058	13
−1 2 0	3.549	3.549	9	2 2 4	1.6058		
1 0 2	3.523	3.523	6	3 0 4	1.5936	1.5935	2
0 1 2	3.494	3.493	6	3 4 1	1.5716	1.5710	2
0 2 1	3.493			−5 0 2	1.5709		
−2 0 2	2.906	2.906	45	−5 2 0	1.5594	1.5593	9
2 2 0/−2 2 0	2.876	2.876	100	5 0 2	1.5482	1.5481	3
2 0 2	2.849	2.848	44	−1 3 4	1.5411	1.5402	1
3 0 0	2.835	2.836	7	−5 1 2	1.5401		
0 2 2	2.762	2.762	79	−4 3 2	1.5259	1.5260	1
−2 1 2	2.723	2.720	6	−2 3 4	1.4742	1.4743	3
−2 2 1	2.711			−4 0 4	1.4528	1.4529	3
1 1 3	2.361	2.360	1	4 4 0	1.4382	1.4382	11
−2 2 2	2.331	2.330	2	−4 1 4	1.4283	1.4285	2
2 2 2	2.301	2.303	3	1 5 2	1.4281		
−3 2 0	2.294	2.294	1	4 0 4	1.4243	1.4242	4
3 0 2	2.273	2.272	1	5 3 0	1.4239		
−3 1 2	2.221	2.221	1	0 4 4	1.3810	1.3810	11
2 3 0	2.220			−2 5 5	1.3808		
0 2 3/0 3 2	2.167	2.167	2	−2 5 2	1.3760	1.3749	1
4 0 0	2.126	2.126	19	−3 4 3	1.3752		
4 1 0	2.051	2.052	1	3 3 4	1.3592	1.3588	1
−4 1 1	1.994	1.992	5	−3 1 5	1.3590		
−3 2 2	1.992			−6 0 2	1.3409	1.3410	2
0 0 4/0 4 0	1.953	1.953	41	0 3 5	1.3398		
−2 3 2	1.939	1.939	3	6 2 0	1.3323	1.3324	3
−3 0 3	1.937			6 0 2	1.3239	1.3240	3
1 0 4/0 1 4/	1.895	1.895	4	0 1 6	1.2844	1.2844	3
0 4 1				−2 3 5/0 6 1	1.2842		
−4 1 2	1.831	1.832	3	−5 1 4	1.2780	1.2782	1
−2 1 4	1.743	1.743	6	2 6 0	1.2448	1.2448	6
2 1 4	1.719	1.718	3	2 0 6	1.2382	1.2383	9
−1 2 4	1.717			−2 1 6	1.2363	1.2363	6
1 2 4	1.705	1.705	3	5 4 2	1.2132	1.2131	4
−4 2 2	1.696	1.696	4	−4 2 5	1.2088	1.2080	3
4 2 2	1.673	1.673	11	5 2 4	1.2079		
−4 0 3	1.663	1.660	13				
5 1 0	1.662						

[a] Unobserved reflections ($I/I_0 < 1\%$) are not listed. [b] The numbers listed are percentages.

ments from 5 to 300 K showed no diamagnetism, which indicated that the compound was not a superconductor.

X-ray and Neutron Diffraction Studies. From the results of powder X-ray diffraction studies, La_2CuSnO_6 was indexed with a monoclinic cell with parameters a = 8.506 (1), b = 7.811 (1), c = 7.814 (1), and β = 91.14 (1)°. The indexed pattern is listed in Table I. The cell size is consistent with a $2a_p \times 2a_p \times 2a_p$ perovskite (Z = 4). A reliable assignment of the space group was not possible from the X-ray diffraction data owing to the inability to positively assign indices to several very weak reflections. It appeared that the reflection conditions were $0k0$ ($k = 2n$) and $h0l$, $00l$ ($l = 2n$), which was consistent with the space group $P2_1/c$ (No. 14).

The most significant result from Rietveld analysis of the X-ray data was that the B and B′ cations had ordered to form $CuO_{4/2}$ and $SnO_{4/2}$ planes. Prior to analysis the structure was expected to be the "ordered perovskite structure" in which the B and B′ cations adopt a rock salt arrangement on the B cation sublattice. This structure was expected because it was known to be the predominant one for ordered $A_2BB'O_6$ perovskites. The difference in the arrangement of B and B′ cations in the expected and observed structures is shown in Figure 2. Another result from the careful examination of powder XRD patterns was that no evidence for a time-dependent solid-state disorder–order transformation was observed. Evidence for a transformation would have been a weak 100 reflection (I/I_0 ~ 10%) that decreased to $I/I_0 < 1\%$ over time.

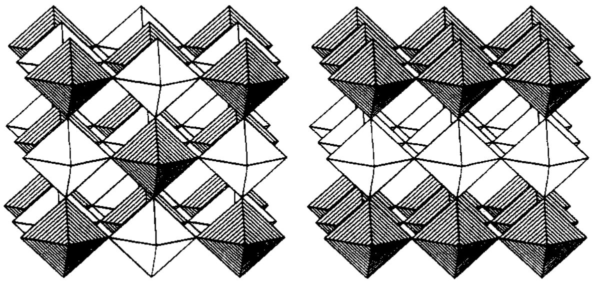

Figure 2. STRUPLO polyhedral representation of the expected (left) and observed (right) ordering scheme of the B and B′ cations for La_2CuSnO_6. The BO_6 octahedra are shaded and the $B'O_6$ octahedra are unshaded. The A cations have been omitted for clarity.

The sensitivity to scattering from the oxygen lattice and superb resolution afforded by neutron diffraction allowed the unambiguous assignment of the −301, 301, −311, 103, −113, 131, and the 113 reflections. This made it immediately clear that $h0l$, $00l$ ($l = 2n$) was not a reflection condition. The reflection condition $0k0$ ($k = 2n$) was still present, which suggested either $P2_1/m$ (No. 11) or $P2_1$ (No. 4) was the correct space group. Rietveld refinement of the neutron diffraction data proceeded in $P2_1/m$ with the layered model from the X-ray refinement. The refinement converged to reliability factors[29] of R_p = 2.4%, R_{wp} = 3.6%,

Table II. Crystallographic Data for La_2CuSnO_6[a]

atom	site	$x/\mathbf{a}$ (σx)	$y/\mathbf{b}$ (σy)	$z/\mathbf{c}$ (σz)	B (σB), Å^2	occupancy
La1	2e	0.2118 (3)	1/4	0.2792 (4)	0.56 (5)	1
La2	2e	0.1978 (3)	1/4	0.7711 (3)	0.50 (4)	1
La3	2e	0.7574 (2)	1/4	0.7855 (3)	0.42 (5)	1
La4	2e	0.7715 (3)	1/4	0.2761 (4)	0.81 (5)	1
Cu1	2a	0	0	0	0.45 (5)	1
Cu2	2c	0	0	1/2	0.43 (5)	1
Sn1	2b	1/2	0	0	0.31 (5)	1
Sn2	2d	1/2	0	1/2	0.24 (6)	1
O1	4f	0.0363 (2)	−0.0329 (3)	0.2498 (3)	0.44 (4)	1
O2	4f	0.2699 (2)	−0.0505 (3)	−0.0476 (3)	0.53 (4)	1
O3	4f	0.2737 (2)	0.0509 (3)	0.5560 (3)	0.65 (4)	1
O4	4f	0.4298 (2)	0.0450 (3)	0.2495 (3)	0.68 (4)	1
O5	2e	0.0274 (4)	1/4	0.0337 (5)	0.64 (6)	1
O6	2e	0.4599 (4)	1/4	−0.0757 (4)	0.73 (6)	1
O7	2e	0.5826 (4)	1/4	0.5237 (4)	0.32 (5)	1
O8	2e	−0.0157 (4)	1/4	0.4706 (4)	0.21 (5)	1

[a] Space group $P2_1/m$ with a = 8.510 (1), b = 7.815 (1), c = 7.817 (1) Å, β = 91.15 (1)°, and Z = 4.

Table III. Models Used for Neutron Diffraction Refinement

space group/ B cation arrangement	R_p[a]	R_{wp}	$R_{\|F\|^2}$	R_{Riet}	R_{exp}	params refined	comments
$P2_1/m$ layered	2.4	3.6	2.8	4.9	1.8	63	$0.21 < B_{iso} < 0.81$ for all atoms
$P2_1$ layered	2.3	3.4	2.3	4.5	1.8	96	B_{iso} for two O atoms was negative; 14 of 17 values that were fixed by symmetry in $P2_1$ were within 3σ of the $P2_1/m$ values
$P2_1/m$ random	2.8	4.1	3.4	5.8	1.8	63	B_{iso} for two of the B cation sites was negative
$P\bar{1}$ rock salt	3.0	4.4	3.6	6.2	1.8	80	B_{iso} for three of four Sn atoms was negative and was 2.49 and 1.91 for two of four Cu atoms

[a] See ref 29 for the definition of the reliability factors. All R values in percent.

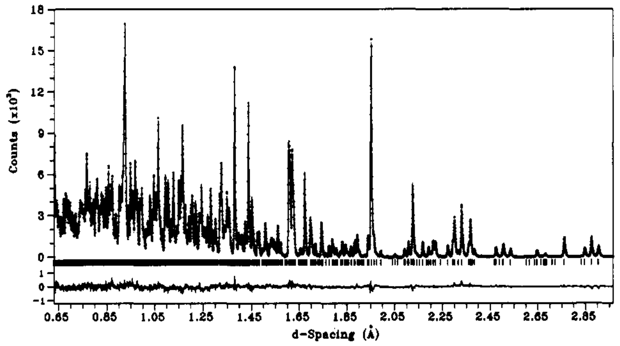

Figure 3. Observed (+), calculated (solid line) and difference (below) neutron diffraction pattern for La_2CuSnO_6 determined at room temperature. The tic marks indicate the allowed reflections in space group $P2_1/m$.

$R_{|F|^2}$ = 2.8%, R_{Riet} = 4.9% with R_{exp} = 1.8% for data from d = 0.633 to 2.967 Å. The atomic parameters are reported in Table II. The observed, calculated and difference patterns along with the allowed reflections are displayed in Figure 3.

Refinement in the noncentrosymmetric space group $P2_1$ converged to slightly lower R values, shown in Table III, but the isotropic temperature factors for two oxygen atoms were negative and the number of parameters refined was increased from 63 to 96. In addition, 14 of 17 positional parameters that were fixed in $P2_1$ refined to within 3 standard deviations of the values in $P2_1/m$. For these reasons the solution in $P2_1/m$ was judged to be more reliable.

Refinements were performed in $P2_1/m$ with a random arrangement of B cations and in $P\bar{1}$ with a rock salt arrangement of B cations. The random model refined to higher R values than the layered model, as indicated in Table III. When the occupation factors for the B cation sites were allowed to vary, they refined to N_{Cu} = 0.92 (3), 0.90 (3), −0.14 (3), and −0.13 (3). These values were quite close to those for the layered model where N_{Cu} = 1, 1, 0, 0.

The refinement with the rock salt model was performed in $P\bar{1}$ because this arrangement of cations was not allowed in $P2_1/m$. The reliability factors were significantly higher for this model, and the temperature factors for five of the eight B and B′ cations were either negative (Sn = −0.07, −0.46, −0.73) or large and positive (Cu = 1.91, 2.49) as noted in Table III.

Additional evidence that the layered model was superior to the rock salt model was provided by Rietveld analysis of the X-ray diffraction patterns generated by these models. The pattern calculated from the rock salt model had too much intensity for the 100, −111, and 111 and 2θ 10.1, 18.7, and 19.0° and too little intensity for the −102, −120, and 102 reflections at 2θ 24.6, 24.8, and 25.0°. The pattern calculated from the layered model matched the observed pattern well. The patterns are displayed in Figure 4.

Discussion

The most significant structural feature of La_2CuSnO_6 is that it contains $CuO_{4/2}$ and $SnO_{4/2}$ layers as opposed to mixed $(Cu_{0.5},Sn_{0.5})O_{4/2}$ layers. Generally, the B and B′ cations in $A_2BB'O_6$ compounds are either ordered in a rock salt arrangement or are disordered. Differences of more than two in charge and more than 0.10 Å between the B and B′ cations strongly favor the ordered rock salt arrangement. With this in mind, our approach to the synthesis of compounds with $BO_{4/2}$ and $B'O_{4/2}$ layers was to use cations that were similar in size and electronegativity, that differed by two in charge, but that were chemically

---

(29) $R_{profile} \equiv 100\sum[|(Y_{obs} - Y_{calc})|]/\sum[|(Y_{obs})|]$; $R_{weighted\ profile} \equiv 100 \times (\sum[W(Y_{obs} - Y_{calc})^2])/\sum[W(Y_{obs})^2])^{1/2}$; $R_{|F|^2} \equiv 100\sum[|(I_{obs} - I_{calc})|]/\sum[|(I_{obs})|]$; $R_{Rietveld} \equiv 100\sum[|(Y_{obs} - Y_{calc})|]/\sum[|(Y_{obs}) - \text{background}|]$; $R_{expected} \equiv 100$ (number of degrees of freedom$/\sum[W(Y_{obs})^2])^{1/2}$. Y_{obs} and Y_{calc} are the observed and calculated profile intensities at a particular time-of-flight value, respectively, and W is the weight of Y_{obs}. I_{obs} and I_{calc} are the observed and calculated intensities of each Bragg peak, respectively.

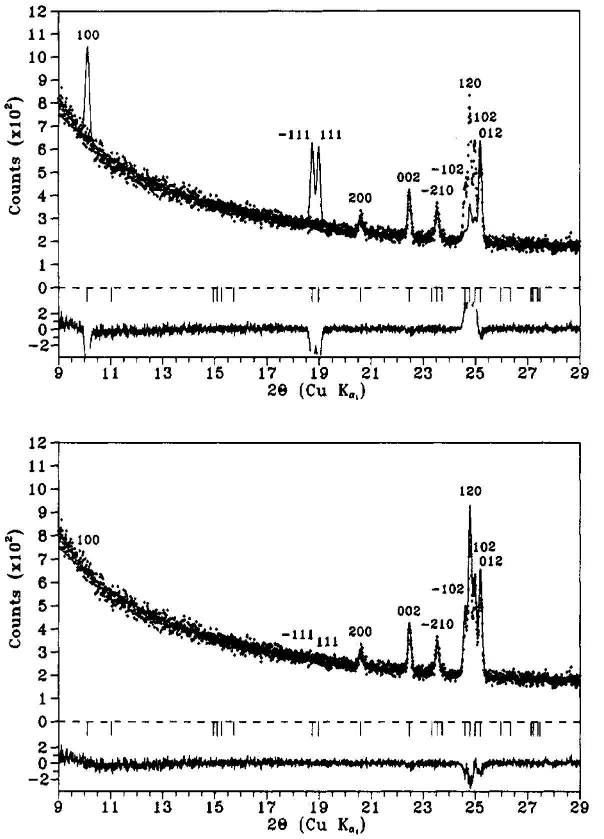

Figure 4. Observed (+), calculated (solid line), and difference (below) X-ray diffraction pattern for La_2CuSnO_6. The calculated patterns were generated by the rock salt model (top) and the layered model (bottom).

dissimilar. Tin(IV) complements copper(II) in these requirements. Tin(IV) has an ionic radius[30] of 0.69 Å with a Pauling electronegativity of 1.96, is d^{10}, and prefers a nearly symmetric environment of anions. Copper(II) has an ionic radius of 0.73 Å with a Pauling electronegativity of 1.90 but is d^9 and frequently undergoes a Jahn–Teller distortion, which leads to four short and two long bonds. In the compound under discussion it is presumed that the similar size and electronegativity of the cations reduced their tendency to order with a rock salt arrangement, and yet their chemical dissimilarity and coordination preferences made a layered arrangement more favorable than a random arrangement.

Other important structural aspects of the compound are that the oxygen octahedra around the Cu and Sn cations are strongly tilted and that the lanthanum cations are displaced toward the negatively charged $CuO_{4/2}$ layer. These effects can be attributed to the mechanism by which perovskite-related compounds commonly optimize their structures, that is, by a distortion of the BO_3 framework that places the A–O bonds under tension and the $BO_{4/2}$ layers under compression. A polyhedral representation of the structure is shown in Figure 5. The tilt of the metal–oxygen framework is denoted $a^-b^+c^-$ in the notation introduced by Glazer.[31] The distortions give rise to two copper, two tin, and four lanthanum sites in the asymmetric unit. The bond distances and angles are presented in Table IV.

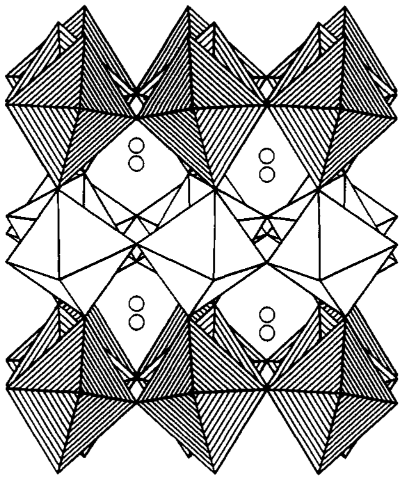

Figure 5. STRUPLO idealized polyhedral representation of La_2CuSnO_6 viewed down the *c* axis. The CuO_6 octahedra are shaded, and the SnO_6 octahedra are unshaded.

Table IV. Bond Distances[a] and Angles for La_2CuSnO_6[b]

Bond Distances			
La1–O5	2.454 (4)	Cu1–O5	1.985 (1) ×2
–O4	2.466 (4) ×2	–O1	1.988 (2) ×2
–O8	2.470 (3)	–O2	2.367 (2) ×2
–O1	2.675 (3) ×2		
–O3	2.708 (3) ×2		
La2–O3	2.389 (3) ×2	Cu2–O8	1.971 (1) ×2
–O6	2.510 (4)	–O1	2.003 (2) ×2
–O5	2.537 (4)	–O3	2.395 (2) ×2
–O1	2.619 (3) ×2		
–O2	2.804 (3) ×2		
–O8	2.941 (4)		
La3–O1	2.461 (3) ×2	Sn1–O2	2.025 (2) ×2
–O7	2.506 (4)	–O6	2.068 (2) ×2
–O2	2.589 (3) ×2	–O4	2.081 (2) ×2
–O6	2.774 (4)		
–O4	2.813 (3) ×2		
–O5	2.977 (4)		
–O8	3.159 (4)		
La4–O8	2.341 (4)	Sn2–O3	2.023 (2) ×2
–O2	2.392 (3) ×2	–O4	2.066 (2) ×2
–O7	2.541 (4)	–O7	2.083 (1) ×2
–O3	2.724 (3) ×2		
–O5	2.915 (4)		
–O1	3.167 (4) ×2		
Bond Angles			
O1–Cu1–O2	89.96 (8)	O2–Sn1–O4	84.86 (9)
O1–Cu1–O5	88.94 (13)	O2–Sn1–O6	88.75 (11)
O2–Cu1–O5	85.80 (12)	O4–Sn1–O6	86.58 (11)
O1–Cu2–O3	88.21 (8)	O3–Sn2–O4	85.02 (9)
O1–Cu2–O8	88.58 (13)	O3–Sn2–O7	83.26 (10)
O3–Cu2–O8	85.42 (10)	O4–Sn2–O7	89.13 (11)

[a] All oxygen atoms within 3.5 Å of the metal atoms are listed. [b] Bond distances in angstroms, and bond angles in degrees.

The lanthanum atom environments will be examined in detail. The coordination numbers for lanthanum atoms 1, 2, 3, and 4 are 8, 9, 10, and 9, respectively, for oxygen atoms within 3.5 Å. The La^{3+} cations are displaced away from the neutral $[SnO_{4/2}]^0$ layers toward the negatively charged $[CuO_{4/2}]^{2-}$ layers. This displacement provides all of the lanthanum atoms with four bonds to the oxygen in the $CuO_{4/2}$ layers. The additional coordination requirements are met by the oxygen atoms in the $LaO_{4/4}$ layer and from the $SnO_{4/2}$ layer. The coordination around each of the lanthanum atoms can be described by three numbers: the first denotes the number of oxygen atoms from the $CuO_{4/2}$ layer, the second the number from the $LaO_{4/4}$ layer, and the third the number from the $SnO_{4/2}$ layer. The coordination of La1 is 4 + 2 + 2, of La2 is 4 + 4 + 1, of La3 is 4 + 2 + 4, and of La4 is 4 + 4 + 1. This notation emphasizes the reduction in coordination number from 12 (4 + 4 + 4) found in cubic perovskites. The lanthanum

---

(30) Shannon, R. D. *Acta Crystallogr.* **1976**, *A32*, 751.

(31) Glazer, A. M. *Acta Crystallogr.* **1972**, *B28*, 3384.

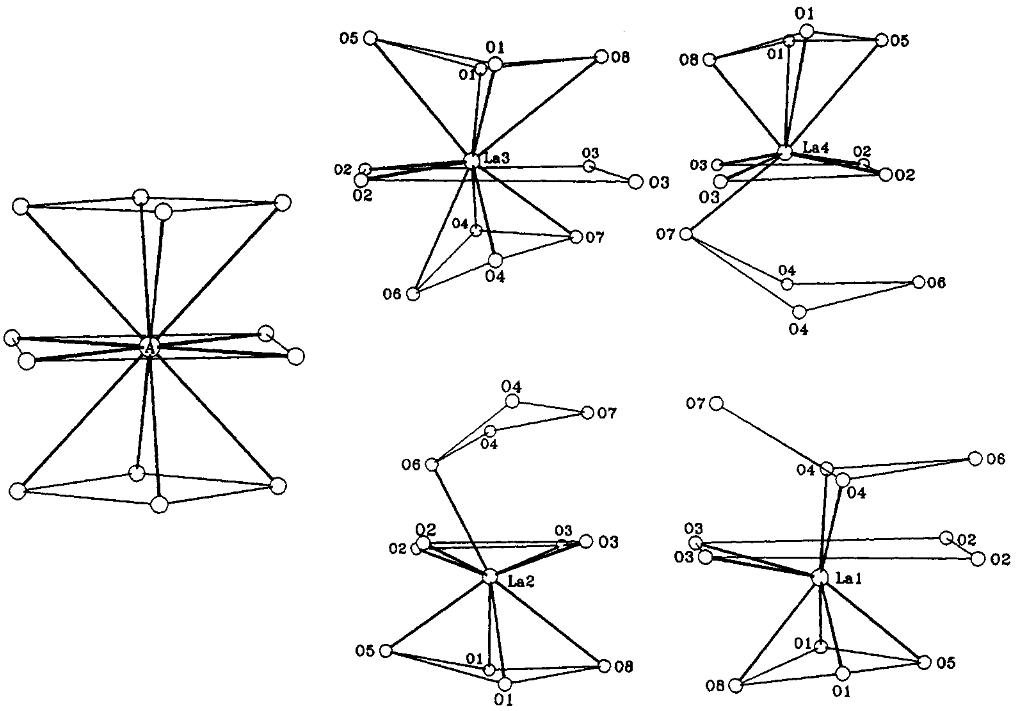

Figure 6. Anionic environment of an A cation in a cubic perovskite (left), and the oxygen atom environment of the La atoms in La_2CuSnO_6. Oxygen atoms within 3.5 Å are denoted by the heavy lines. The lines connecting the oxygen atoms are to emphasize the atoms from the $CuO_{4/2}$ (O1, O5, O8), the $LaO_{4/4}$ (O2, O3), and the $SnO_{4/2}$ (O4, O6, O7) layers.

environments are shown in Figure 6.

Several aspects of the metal–oxygen framework will now be discussed. The coordination around the tin atoms is close to octahedral. The coordination around copper is less regular; a Jahn–Teller distortion has caused four short and two long bonds. Presumably a cooperative Jahn–Teller distortion, in which all of the copper d_{z^2} orbitals are aligned parallel to the a axis, has caused the 0.7-Å expansion of the unit-cell parameter in the a direction.

The in-plane Sn–O bond distances are longer (2.06 Å average) than the in-plane Cu–O bond distances (1.99 Å average). As a result the oxygen atoms in the tin–oxygen plane displaced much further from their ideal positions than the oxygen atoms in the copper–oxygen plane. The Sn–O bond distances are very similar to those seen in other tin oxides (2.05 Å).[32] The Cu–O bond distances are slightly longer than are observed in the highly covalent copper–oxygen planes in high-temperature superconductors. For example, the in-plane bond lengths for $YBa_2Cu_3O_{6.81}$[5b] are 1.928 (1) and 1.962 (1) Å. The displacements of the oxygen atoms, which occur due to the tension of the La–O bonds and the mismatch of the in-plane Cu–O and Sn–O bonds, put the $CuO_{4/2}$ and $SnO_{4/2}$ planes under compression and buckle the layers. The buckling of the layers can be seen in Figure 7.

The distances of the long Cu–O bonds, 2.395 (2) and 2.367 (2) Å, are typical for Jahn–Teller copper. At this time the effect of the Jahn–Teller distorted copper and the low overall symmetry (monoclinic) on the electronic properties of La_2CuSnO_6 is not clear. The material is very dark but has a brown cast and is therefore expected to be a semiconductor. Further work is in progress to determine the effect of the substitution of alkaline-earth-metal elements for lanthanum on the crystallographic and physical properties of this compound.

The phase diagram study was done primarily to determine whether any other compounds with Cu:Sn ratios other than 1:1 existed. We found no evidence for other ternary phases. The determination of the phase relationships helped us explain why the substitution of smaller rare-earth-metal cations or larger tetravalent B′ cations was unsuccessful.

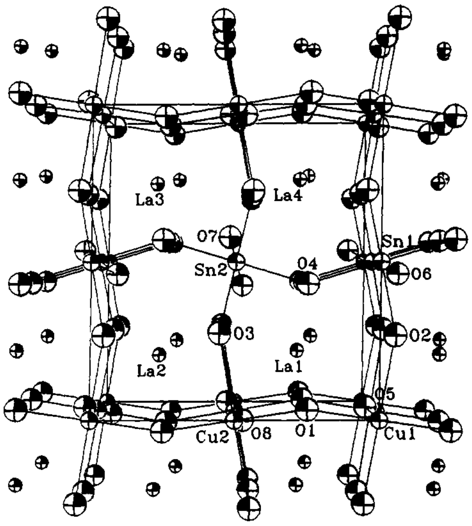

Figure 7. ORTEP of La_2CuSnO_6 viewed down the *b* axis. The unit cell is outlined.

The diagram shows that the formation of La_2CuSnO_6 is in competition with the formation of La_2CuO_4[21] (distorted K_2NiF_4 structure), $La_2Sn_2O_7$[26] (pyrochlore structure), and CuO[33] (PtS structure). The competition can be quantified in terms of the Goldschmidt[34] tolerance factor, which has been adapted for $A_2BB'O_6$ compounds:

$$t = (r_A + r_O)/\sqrt{2}(((r_B + r_{B'})/2) + r_O)$$

---

(32) Brisse, F.; Knop, O. *Can. J. Chem.* **1968**, *46*, 859.

(33) Åsbrink, S.; Norrby, L.-J. *Acta Crystallogr.* **1970**, *B26*, 8.

(34) Goldschmidt, V. M. *Str. Nor. Vidensk-Akad. Oslo* **1926**, *1*, 1.

(35) Ramadass, N.; Gopalakrishnan, J.; Sastri, M. V. C. *J. Inorg. Nucl. Chem.* **1977**, *40*, 1453–1454.

(36) Blasse, G. *J. Inorg. Nucl. Chem.* **1965**, *27*, 993–1003.

482 *Chem. Mater.* **1991,** *3,* 482-486

Table V. Tolerance Factors for Several $A_2^{3+}CuB^{4+}O_6$ Compounds for Which A_2CuO_4, $A_2B'_2O_7$, and CuO Compounds Also Exist

compd	*t*	sym	ref
$La_2CuTiO6$	0.950	pseudocubic	35
$La_2CuIrO6$	0.945	monoclinic	36
$La_2CuSnO6$	0.930	monoclinic	this work
"La_2CuZrO_6"[a]	0.923		this work
"$La_{1.5}Nd_{0.5}CuSnO_6$"[b]	0.922		this work
"La_2CuPbO_6"[a]	0.911		this work
"Nd_2CuSnO_6"[a]	0.899		this work

[a] Mixture of A_2CuO_4, $A_2B'_2O_7$, and CuO. [b] Mixture of La_2CuSnO_6, Nd_2CuO_4, $Nd_2Sn_2O_7$, and CuO.

where r_A, r_O, r_B, and $r_{B'}$ are the ionic radii[30] of the ions. The tolerance factor for La_2CuSnO_6 is 0.930. Attempts to decrease *t* by the substitution of the slightly smaller Nd^{3+} ion (1.27 Å) for the La^{3+} ion (1.36 Å) or the slightly larger Zr^{4+} ion (0.73 Å) or Pb^{4+} ion (0.78 Å) for Sn^{4+} ion 0.69 Å) result in the formation of $A_2B'_2O_7$, A_2CuO_4, and CuO. The lower limit of the tolerance factor for these types of systems seems to be between 0.930 and 0.923. The tolerance factors for these and two other compounds are listed in Table V. It appears that when $t < 0.930$, it is energetically unfavorable to further compress the $CuO_{4/2}$ and $B'O_{2/4}$ layers to bring oxygen atoms within A–O bonding distances and that the reactants form the three competing phases.

Conclusions

The synthesis of layered cuprates is an important goal because of their relationship to high-temperature cuprate superconductors. The synthesis of layered cuprates that are stoichiometric in oxygen is limited by several factors, however, which include the energetic favorability of ordering B cations between AO_3 layers and strong competition from phases that are energetically similar. La_2CuSnO_6 is an example of a compound in which these factors have been overcome.

Acknowledgment. This work benefitted from the use of the Intense Pulsed Neutron Source at Argonne National Laboratory with funding provided by the National Science Foundation and the Science and Technology Center for Superconductivity (NSF-DMR-8809854). We thank R. Hitterman, J. Jorgenson, and F. Rotella for their assistance with the neutron diffraction experiment. We gratefully acknowledge J. P. Thiel for his assistance with the refinement programs and helpful discussions and J. T. Vaughey for his helpful discussions. We also acknowledge the Northwestern Materials Research Center for support of the X-ray Diffraction Facility (MRL-DMR-8821571).

High-Field ^{11}B Magic-Angle Spinning NMR Characterization of Boron Nitrides

Paul S. Marchetti,[†] Daekeun Kwon,[‡] Wayde R. Schmidt,[§] Leonard V. Interrante,[‡]
and Gary E. Maciel*,[†]

Department of Chemistry, Colorado State University, Fort Collins, Colorado 80523;
Department of Chemistry, Rensselaer Polytechnic Institute, Troy, New York 12180-3590; and
Department of Materials Engineering, Rensselaer Polytechnic Institute,
Troy, New York 12180-3590

Received November 16, 1990. Revised Manuscript Received March 25, 1991

High-field (14.0 T) ^{11}B magic-angle spinning NMR characterization of the major forms of boron nitride reveals differences between the cubic (c-BN) and hexagonal (h-BN) forms, in terms of both isotropic chemical shifts and magnitude of the second-order quadrupole contribution to observed NMR line shapes. ^{11}B NMR spectra of the pure turbostratic (t-BN) form and of t-BN in the form of an AlN/BN composite are indistinguishable from those of crystalline h-BN. This observation is in accord with the weak nature of the interplanar bonding interaction in t-BN. The results presented herein involving the structural characterization of boron nitrides by solid-state NMR should serve as a foundation for future studies involving pyrolytic conversion of organometallic and polymeric precursors to boron nitride.

Introduction

High-field solid-state NMR spectroscopy with magic-angle spinning (MAS) has proven to be a highly useful technique for the direct, yet nondestructive, characterization of crystalline inorganic oxides, including various silicates,[1] aluminosilicates[1-7] (especially zeolites), SiAlONs,[8,9] and oxynitrides.[3,10] Moreover, considerable progress has been made recently in applying this technique to the identification of high-performance non-oxide ceramic materials such as SiC,[3,11] Si_3N_4,[3,11,12] and AlN,[13,14] as well as to the study of pyrolytic conversion of organometallic precursors to these materials.[15-17] Among the

---

[†] Colorado State University.

[‡] Department of Chemistry, Rensselaer Polytechnic Institute.

[§] Department of Materials Engineering, Rensselaer Polytechnic Institute.

(1) Magi, M.; Lippmaa, E.; Samoson, A.; Engelhardt, G.; Grimmer, A. R. *J. Phys. Chem.* **1984,** *88,* 1518–1522.

(2) Fyfe, C. A.; Gies, H.; Feng, Y. *J. Am. Chem. Soc.* **1989,** *111,* 7702–7707.

(3) Turner, G. L.; Kirkpatrick, R. J.; Risbud, S. H.; Oldfield, E. *Am. Ceram. Soc. Bull.* **1987,** *66,* 656–663.

(4) Fyfe, C. A.; Gobbi, G. C.; Hartmann, J. S.; Lenkinski, R. E.; O'-Brien, J. H.; Beange, E. R.; Smith, M. A. R. *J. Magn. Reson.* **1982,** *47,* 168–173.

(5) Lippmaa, E.; Magi, M.; Samoson, A.; Engelhardt, G.; Grimmer, A. R. *J. Am. Chem. Soc.* **1980,** *102,* 4889–4893.

(6) Thomas, J. M.; Bursill, L. A.; Lodge, E. A.; Cheetham, A. K.; Fyfe, C. A. *J. Chem. Soc., Chem. Commun.* **1981,** 276–277.

(7) Klinowski, J.; Thomas, J. M.; Audier, M.; Vasudevan, S.; Fyfe, C. A.; Hartman, J. S. *J. Chem. Soc., Chem. Commun.* **1981,** 570–571.

0897-4756/91/2803-0482$02.50/0